Applied Acoustics 135 (2018) 22–28

Contents lists available at ScienceDirect

Applied Acoustics

journal homepage: www.elsevier.com/locate/apacoust

Application of ultrasonic vibrations for minimization of the accumulation of limescale in steam irons

Hasan Koruk[a,*], Muzaffer Serenli[b], Kenan Y. Sanliturk[c]

[a] MEF University, Mechanical Engineering Department, 34396 Istanbul, Turkey
[b] Silter İleri Ütüleme Sistemleri Sanayi ve Ticaret Ltd. Şti., Büyükçekmece, 34535 Istanbul, Turkey
[c] Istanbul Technical University, Mechanical Engineering Department, 34437 Istanbul, Turkey

ARTICLE INFO

Keywords:
Ultrasonics
Ultrasonic cleaning
Limescale
Steam iron
Finite element model
Laser vibrometer

ABSTRACT

The accumulation of limescale in steam irons can significantly reduce the ironing efficiency. It is this problem that inspired us to introduce ultrasonic vibrations to irons in order to minimize limescale accumulation. This study describes a methodology for designing, modelling and optimizing an iron fitted with an ultrasonic exciter in an attempt to minimize limescale accumulation. In our methodology, first, an experimental demonstration of the potential benefits of ultrasonic vibrations in steam irons was conducted, using two existing irons, one of which was equipped with an ultrasonic exciter. Having confirmed the benefits, an experimental iron was designed and then optimized to maximise ultrasonic vibrations using finite element analyses within a predefined frequency range. To validate the results of the finite element analyses, a prototype iron base was built, and forced vibrations of this prototype, at ultrasonic frequencies ranging from 35 to 40 kHz, were measured using a laser vibrometer. The results of the theoretical and experimental vibration analyses as well as the physical experiments on the steam irons indicate that it is possible for ultrasonic vibrations to be utilized in irons to minimize the accumulation of limescale.

1. Introduction

Steam irons are used in almost every home for removing wrinkles from clothes. However, when the water in an iron evaporates, calcite (calcium carbonate) tends to form a layer of limescale on various surfaces, such as in the steam generating chambers and on the surfaces of the steam passageways. This leads to inefficiencies in performance. Understanding how to minimize limescale accumulation in devices and machines, including both domestic and industrial steam irons, is an ongoing challenge [1]. Ultrasonic vibrations are being used in many existing technologies [2–10], for cleaning surfaces, such as on 3D printed objects [11] and during water filtration [12]. The inspiration for using ultrasonic vibrations in irons to minimize the accumulation of limescale arose from observing the existing diverse technologies and applications that use ultrasonic vibrations, especially for cleaning processes.

Although the analytical prediction of the dynamic properties of complex structures, especially at ultrasonic frequencies, is quite difficult, it is possible to use finite element analyses to design and optimize the ultrasonic vibrations of such complex structures [13]. However, finite element models often need to be followed by experimental verifications. Laser Doppler vibrometers, on the other hand, are capable of measuring the ultrasonic vibrations of complex structures, and can therefore be used to provide the necessary experimental verifications [14]. The literature contains a number of studies which have drawn upon finite element analysis and laser Doppler vibrometry when designing ultrasonic technologies. For example, Waldron et al. [15] used finite element analysis and laser Doppler vibrometry to identify damage in beams. Vasiljev et al. [16] utilized finite element simulations and laser Doppler vibrometers to design an ultrasonic system for solar panel cleaning. Furthermore, Yin et al. [17] recently used finite element methods to simulate an ultrasonic de-icing process.

This paper presents a methodology for designing, modelling and optimizing a steam iron to vibrate within a predefined ultrasonic frequency band so as to minimize the accumulation of limescale on its surfaces. To the best knowledge of the authors, this is the first study in the literature, which deals with modelling and optimizing ultrasonic vibrations in irons which includes prototyping and testing. The main objectives of this study are: (i) to use experimental demonstration to show that the use of ultrasonic vibrations in steam irons can reduce the accumulation of limescale; (ii) to design and optimize a steam iron base with an appropriate ultrasonic exciter using finite element analyses;

* Corresponding author.
E-mail addresses: korukh@mef.edu.tr (H. Koruk), mserenli@silter.com.tr (M. Serenli), sanliturk@itu.edu.tr (K.Y. Sanliturk).

https://doi.org/10.1016/j.apacoust.2018.01.024
Received 3 November 2017; Received in revised form 26 January 2018; Accepted 30 January 2018

and (iii) to create a prototype of the optimized iron base from which to measure the forced vibrations at ultrasonic frequencies in order to validate the design.

2. Designing an ultrasonic steam iron

Ultrasonic vibrations are already being used in ultrasonic cleaning to remove contaminants [11]. By utilising the same principles, we believe that ultrasonic vibrations can be used in steam irons to minimize the accumulation of limescale. However, when designing an ultrasonic iron, various challenges need to be overcome. For example, one must ensure that the ultrasonic vibrations do not cause discomfort to the end user. The vibration-induced noise should not be audible to the user, therefore, the frequency of vibrations must be higher than 20 kHz, the upper limit of the audible frequency range for humans. Moreover, the ultrasonic exciter used to create vibrations within the iron must be small enough to be installed directly, but powerful enough to create the necessary vibrations. Furthermore, as the exciter contains sensitive components, i.e., piezoelectric ceramics, it must be protected against excessive temperatures.

2.1. Preliminary ultrasonic iron design

In order to develop an "ultrasonic iron" with its own ultrasonic exciter, a preliminary design based on a typical steam iron was created. The design comprised the main body of an iron, including a steam generating chamber, steam passageways and rear chamber, as well as a floor panel with an added ultrasonic exciter, shown in Fig. 1a. A prototype of this ultrasonic iron was built and experiments conducted to verify the expectation that ultrasonic vibrations are indeed beneficial in reducing the accumulation of limescale. Physical experiments were carried out using two steam irons, one with and one without an ultrasonic exciter. The duration of the experiments was a total of ten hours a day over a four-week period. During these experiments, the ultrasonic exciter was set at around 35 kHz. At the end of the experimental period, photographs of limescale accumulation in both irons were taken. These are presented in Fig. 1b and c. In these photographs, one can clearly observe there is significantly less limescale on the surfaces of the iron which were exposed to ultrasonic vibrations (approximately 32% less).

Having obtained experimental evidence that ultrasonic vibrations can indeed decrease the accumulation of limescale in steam irons, we decided to optimize the dynamic behaviour of the iron structure so as to generate effective ultrasonic vibrations at the specific locations where limescale had been seen to accumulate. To do this, a finite element model of the prototype ultrasonic iron was developed so its modal behaviour could be predicted at ultrasonic frequencies. The ultrasonic exciter in the iron was modelled using 20-noded solid elements, and the main body of the iron and the floor panel were modelled using quadratic 10-noded solid elements. This initial finite element model consisted of around 540 k elements and 930 k nodes in total. Each individual part was assumed to be "welded" to the matching surfaces. After the model creation, the eigenvalue problem given by

$$\mathrm{K}\boldsymbol{\phi} = \omega^2 \mathrm{M}\boldsymbol{\phi} \tag{1}$$

was solved to determine the natural frequencies, $f_i = \frac{\omega_i}{2\pi}$ and mode shapes, $\boldsymbol{\phi}_i$ of the iron assembly. Here, K and M are the stiffness and mass matrices of the iron assembly, respectively, and i denotes the mode number.

The finite element model predicted 170 modes up to 40 kHz and the first four mode shapes of the iron are presented in Fig. 2, the corresponding natural frequencies being $f_1 = 1223$ Hz, $f_2 = 1785$ Hz, $f_3 = 2298$ Hz and $f_4 = 3785$ Hz, respectively. From these analyses, it became clear that the lowest natural frequencies, other than those for the rigid body modes, were much lower than the lower limit of the ultrasonic frequencies.

The natural frequencies predicted by this model at ultrasonic frequencies and the corresponding mode shapes were also examined. For the purposes of illustration, some of the mode shapes with natural frequencies greater than 30 kHz are presented in Fig. 3. The predicted results of the preliminary design indicated that the mode shapes at ultrasonic frequencies mostly comprised local modes due to local flexibilities in the iron structure. It is worth restating that the main purpose here is to prevent the accumulation of limescale at various locations of irons, including in the steam generating chamber where water droplets evaporate and turn into steam, on the surfaces of steam passageways, and in the rear chamber. Examination of the mode shapes of the preliminary design indicated that this design needed to be improved in order to create effective ultrasonic vibrations at the desired locations in the iron. Consequently, we decided to revise and optimize the current iron structure to create more effective ultrasonic vibrations in order to achieve less limescale accumulation.

2.2. Optimization of the ultrasonic iron for effective ultrasonic vibrations

Undoubtedly, the most critical component of an ultrasonic iron is the ultrasonic exciter. Therefore, the exciter must be designed, carefully analysed and skilfully incorporated into the overall iron structure. In this investigation, we designed a piezoelectric-type ultrasonic exciter with a working frequency range of 35–40 kHz. A thermal isolator between the piezoelectric ceramics and the iron surface was placed to avoid excessive heating of the piezoelectric exciter. A conical-shaped part was used to assemble the piezoelectric ceramics with the ceramic thermal isolator, and the iron head was used to connect the exciter to the iron body, as shown in Fig. 4a. Electrodes were added to provide input electrical energy to the piezoelectric ceramics. The material properties of all these components are listed in Table 1, including Young's modulus (E), density (ρ), and Poisson's ratio (ν).

Once the physical design was completed, a finite element model of the exciter was created in free-free conditions to predict the natural frequencies and mode shapes of the exciter system. Using the finite element analysis, the ultrasonic exciter was tuned so as to set its first natural frequency in correspondence with the "tension-compression"

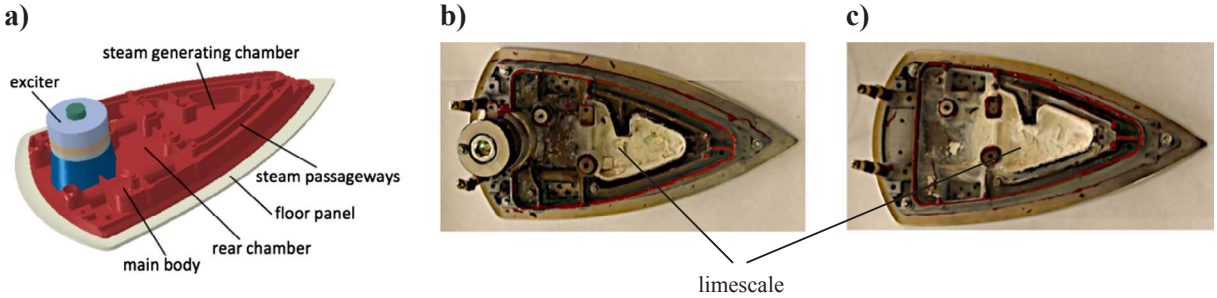

Fig. 1. The preliminary ultrasonic iron design, including the main body of the iron, floor panel and exciter (a); photograph of limescale accumulation for the iron with ultrasonic excitation (b); and photograph of the iron without ultrasonic excitation (c) taken after the experiments.

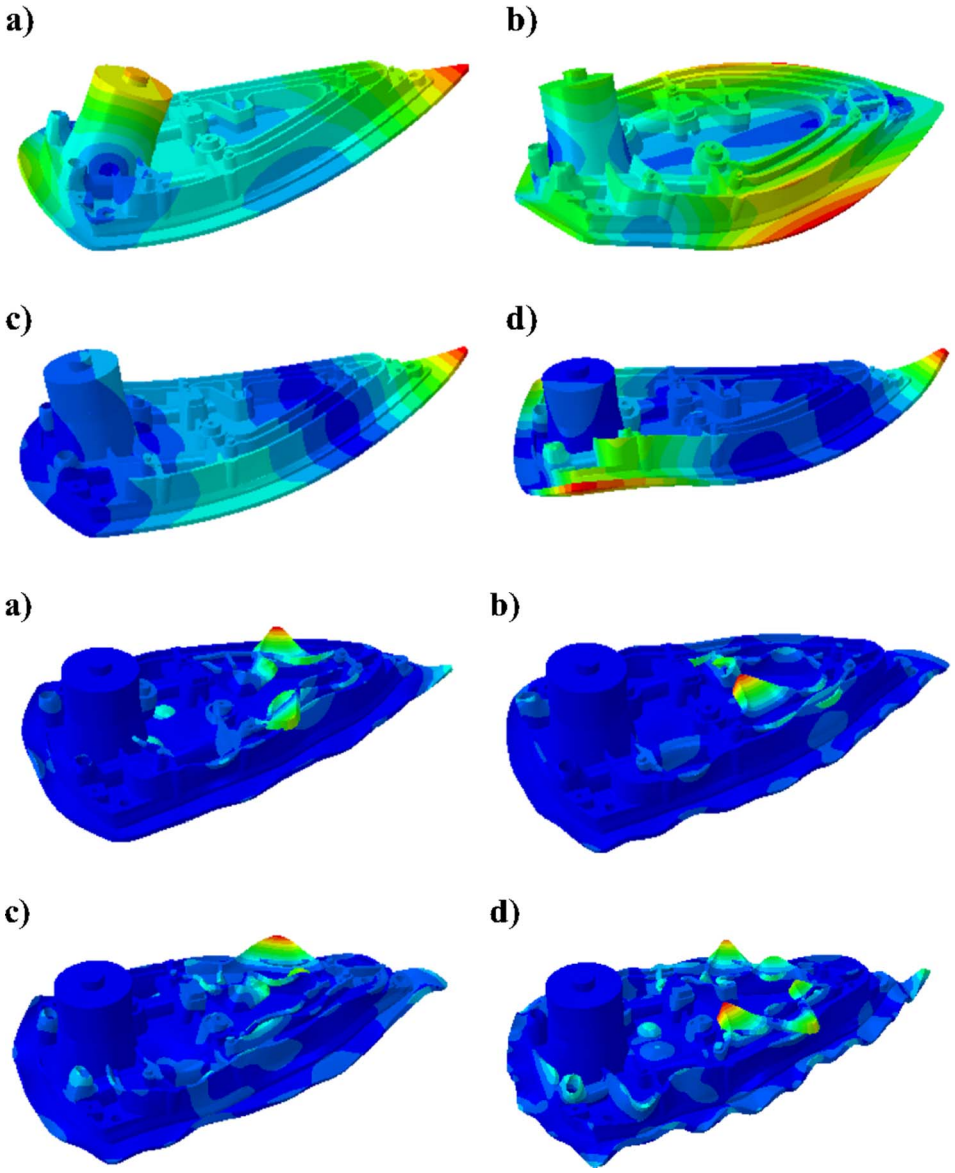

Fig. 2. The first four mode shapes of the preliminary ultrasonic iron (a-d) which were predicted using the finite element model.

Fig. 3. Sample mode shapes at ultrasonic frequencies predicted using the finite element model: (a) $f = 31.1$ kHz, (b) 32.6 kHz, (c) 34.2 kHz and (d) 39.3 kHz.

mode to be sit as close as possible to the desired working frequency. The tension-compression mode, which was predicted at 38.2 kHz, is shown in Fig. 4b. With this information, a prototype of the ultrasonic exciter was built. When tested, using the impedance test method, the natural frequency of the exciter was identified as 37.8 kHz.

The next step was to incorporate the ultrasonic exciter into the iron and then optimize the iron structure to create effective vibrations at ultrasonic frequencies. Thermal aspects of the iron's materials were

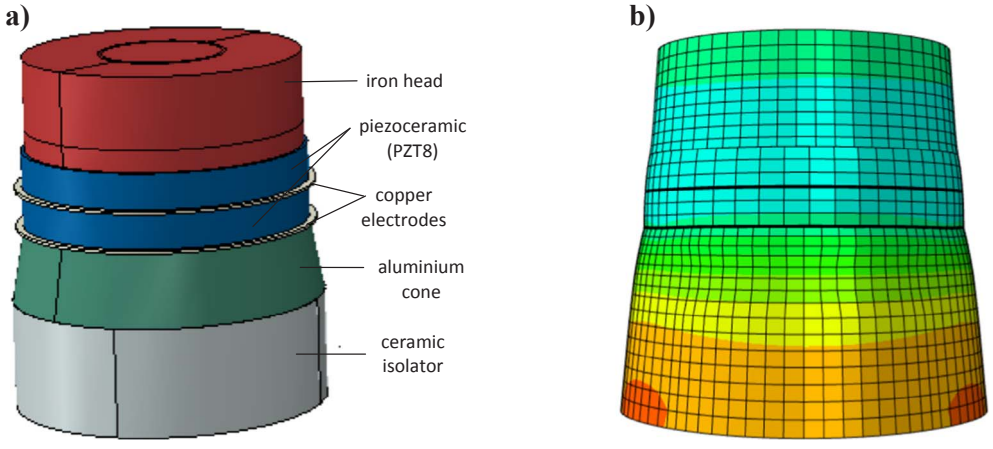

Fig. 4. (a) The model of the piezoelectric exciter with ceramic isolator and (b) its first tension-compression mode at $f = 38.2$ kHz predicted using the finite element model.

Table 1
Material properties of the components of the piezoelectric exciter.

Component	E (GPa)	ρ (kg/m^3)	ν
Iron head	178.5	7113.6	0.30
Piezoelectric ceramic (PZT8)	72.7	6840.0	0.31
Copper electrode	93.5	8171.5	0.30
Aluminium cone	59.5	2462.4	0.33
Ceramic isolator	90.0	2869.3	0.31

taken into account. Then the materials for the main body and floor panel were selected to be Etial 150 and Al 6082, respectively. Young's modulus, density, and Poisson's ratio for these aluminium-based materials are $E = 70$ GPa, $\rho = 2950\,\text{kg/m}^3$ and $\nu = 0.33$. As presented in the previous section, the preliminary design was not quite right, as it was not creating effective ultrasonic vibrations in the steam generating chamber, steam passageways, or the rear chamber. During observations that the central part of the steam iron did not vibrate effectively at ultrasonic frequencies (Fig. 3) and, as seen in Fig. 1b, this was leading to the accumulation of limescale there. In order to rectify this, the preliminary design needed to be modified to improve vibrations at ultrasonic frequencies within the iron in the areas where limescale was accumulating. It should be noted that any reduction in the thickness of the main body adversely affects the heat capacity of the iron, and this may lead to undesirable vibrations below ultrasonic frequencies. Due to this, we decided to create a circular plate section on the iron body, as illustrated in Fig. 5a, so as to maximize the ultrasonic vibrations at desired locations in the iron while keeping the heat capacity of the iron almost unchanged. We decided on the location of the circular plate by taking into consideration from where the water in the iron is injected or sprayed onto the hot base plate to generate steam. The initial thickness and the radius of the circular plate yielding the desired natural frequency were predicted using an analytical model which assumed rigid boundary conditions. The natural frequency, f, was determined using

$$\lambda^2 = 2\pi f r^2 \sqrt{\frac{\rho h}{D}} \tag{2}$$

where r and h are the radius and thickness of the plate, D is the flexural rigidity of the plate, and λ^2 is a frequency parameter given in the literature for different values [18]. The flexural rigidity is given by

$$D = \frac{Eh^3}{12(1-\upsilon^2)} \tag{3}$$

The natural frequencies estimated via this simple analytical approach, for $r = 15$ mm and for different thickness values of the circular plate, are plotted in Fig. 5b. This shows that a circular plate with a thickness of 4 mm and a radius of 15 mm is suitable for the targeted frequency range (i.e., 35–40 kHz). Before creating a finite element model for an iron with a specified circular plate section, natural frequencies of a circular plate with rigid boundary conditions predicted by analytical approach were compared with the finite element predictions using shell and solid elements. For the mode of interest, depicted in Fig. 5c, such comparisons revealed that for $r = 15$ mm and $h = 4$ mm the predicted natural frequencies are very close: 38.0 kHz via the shell finite element model; 38.5 kHz via the solid finite element model; and 38.8 kHz via the analytical model.

These calculations suggested that a circular plate section with appropriate dimensions could be created in the steam generating chamber so that this section could be effectively excited by the ultrasonic exciter. This possibility was simulated using a finite element model of an iron, including the exciter and the circular plate section. Furthermore, the findings gathered from the analyses of the preliminary model were also incorporated into the finite element model. Some stiffeners were added to increase the stiffness of the shells on the iron body to prevent local modes caused by local flexibilities in the iron. The position of the exciter was also slightly modified in order to accommodate some of the existing electronic components of the iron. This led to us carrying out further simulations to assess the suitability of the different design options and to confirm that the objectives could be achieved in the final design. The final finite element model of the iron had about 800 k finite elements in total.

The natural frequencies and corresponding mode shapes for the final, optimized iron structure were predicted. It should be stated that comparing the natural frequencies and modes shapes of the older and the optimized structure revealed that both the natural frequencies and mode shapes were quite different from each other. The mode shapes corresponding to natural frequencies within the frequency range of interest (i.e., 35–40 kHz), presented in Fig. 6, suggested that the vibrations within 35–40 kHz could be quite effective in the steam generating chamber, steam passageways, and the rear chamber compared to the preliminary situation shown in Fig. 3. It is worth restating that these locations are where lime particles are mostly seen to accumulate. The predicted mode shapes in Fig. 6 also implied that a narrow band excitation could create effective vibrations at the desired locations. For example, sweeping in a frequency range (e.g., 35–37 kHz) can provide effective ultrasonic vibrations at all the desired regions in the iron. In an effort to verify the predictions, a test rig was developed and ultrasonic vibration measurements on a prototype iron were carried out. The next section describes the experimental work and the associated results.

3. Verification using operational deflection shapes

For the purpose of design verification, a prototype iron was built and forced vibrations of this prototype at ultrasonic frequencies were measured using a laser vibrometer. Although the bottom surface of the iron touches a surface when it is in use, the vibration tests were performed in free-free conditions due to the advantages it offers when experimental and theoretical results are to be compared [13]. This approach is justifiable, as the vibration modes at ultrasonic frequencies are not expected to be significantly affected when the iron is moved over a surface with a relatively very flexible foundation during the ironing operation. The excitation unit of the iron prototype was driven using a control unit and a scanning laser vibrometer (PSV-400 Scanning Vibrometer, Polytec GmbH, Germany) was used to measure the

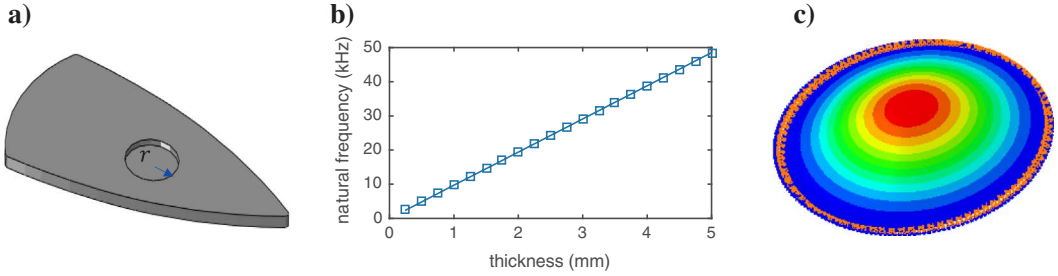

Fig. 5. (a) The circular plate section, (b) variation of the analytical natural frequency with respect to thickness for a sample circular plate with $r = 15$ mm, and (c) the mode shape of the circle with $r = 15$ mm and $h = 4$ mm predicted using the finite element model.

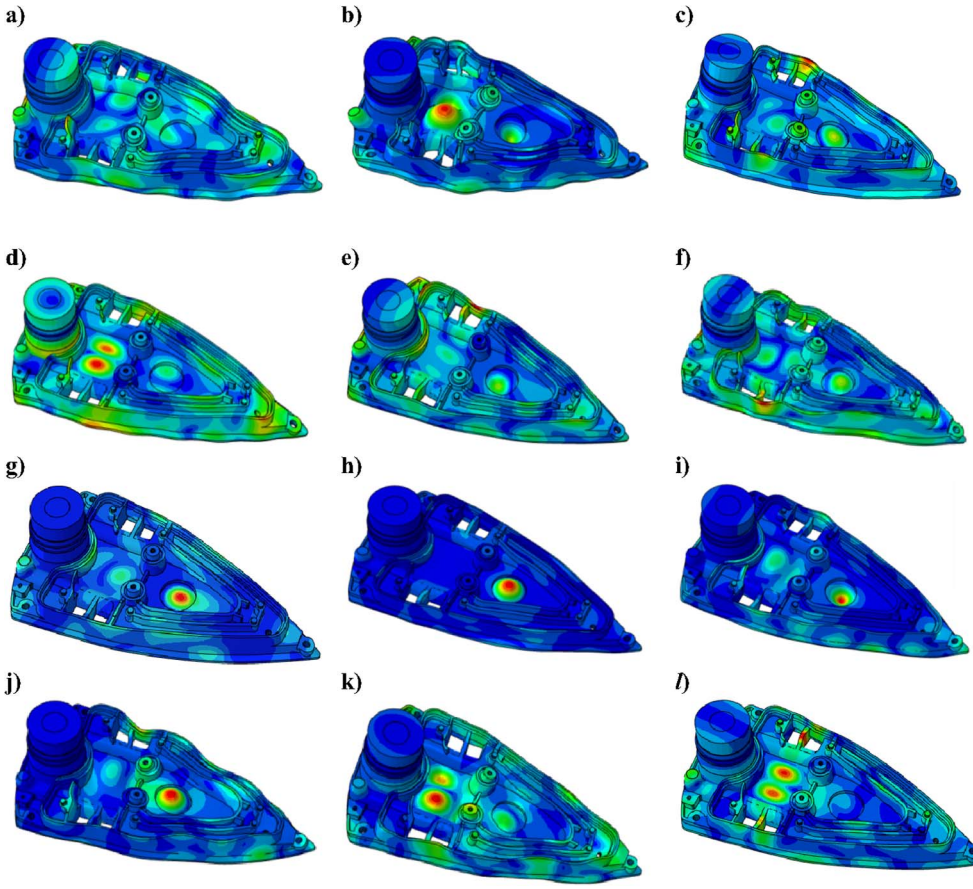

Fig. 6. The vibration mode shapes predicted using the finite element model at frequency f being (a) 34.93 kHz, (b) 35.28 kHz, (c) 35.62 kHz, (d) 35.73 kHz, (e) 36.18 kHz, (f) 36.41 kHz, (g) 36.53 kHz, (h) 36.78 kHz, (i) 36.90 kHz, (j) 37.14 kHz, (k) 37.22 kHz and (*l*) 39.85 kHz.

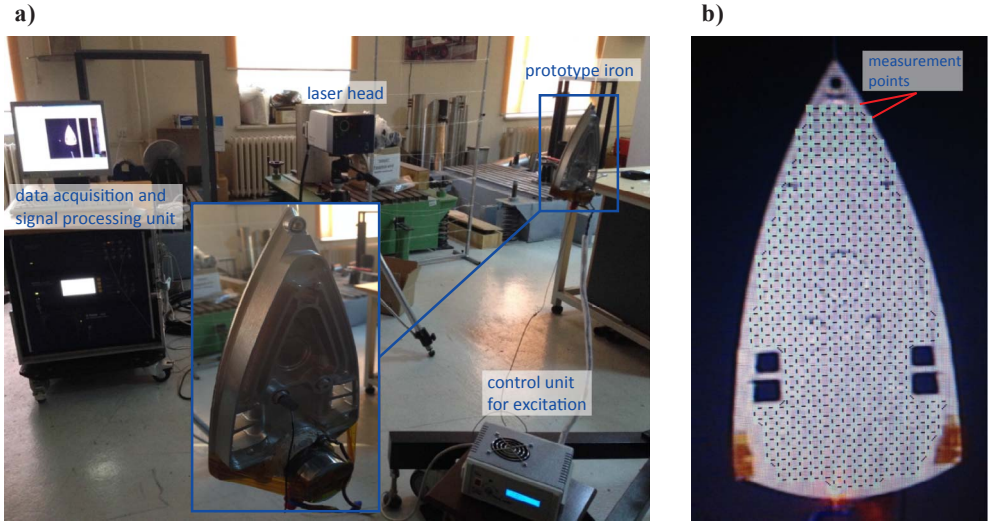

Fig. 7. (a) The experimental setup including the prototype steam iron with the excitation unit, the control unit for excitation, the laser head, and the data acquisition/signal processing unit of the laser vibrometer, and (b) the laser measurement points.

corresponding vibrations at 476 grid points on the back of the iron. The experimental setup and the response locations are depicted in Fig. 7. The main purpose of these tests was to excite the system at different frequencies and measure the responses at grid points in order to determine the operational deflection shapes, expected to be similar to the mode shapes at or around natural frequencies. The excitation frequency was varied from 35 to 40 kHz.

The measured operational deflection shapes are presented in Fig. 8. The results clearly indicated that the ultrasonic exciter, specifically designed for this test, effectively excited the system and created ultrasonic vibrations within 35–40 kHz.

In order to verify finite element predictions, the measured operational deflection shapes were visually compared to the predicted mode shapes. For example, the measured operational deflection shape at 35 kHz in Fig. 8a is quite similar to the estimated mode shape at 35.3 kHz in Fig. 6b. Similarly, the measured operational deflection shape at 36 kHz in Fig. 8b is very similar to the estimated mode shape at 35.7 kHz in Fig. 6d. In general, the identified operational deflection shapes indicate that the steam generating chamber, steam passageways and the iron bottom plate vibrate effectively at ultrasonic frequencies as predicted by the numerical model. Finally, it should be noted that this is not a finalized project yet. More research needs to be carried out before an ultrasonic iron can become a reality. Although, the main body, i.e., base plate, of a steam iron is optimized for effective ultrasonic

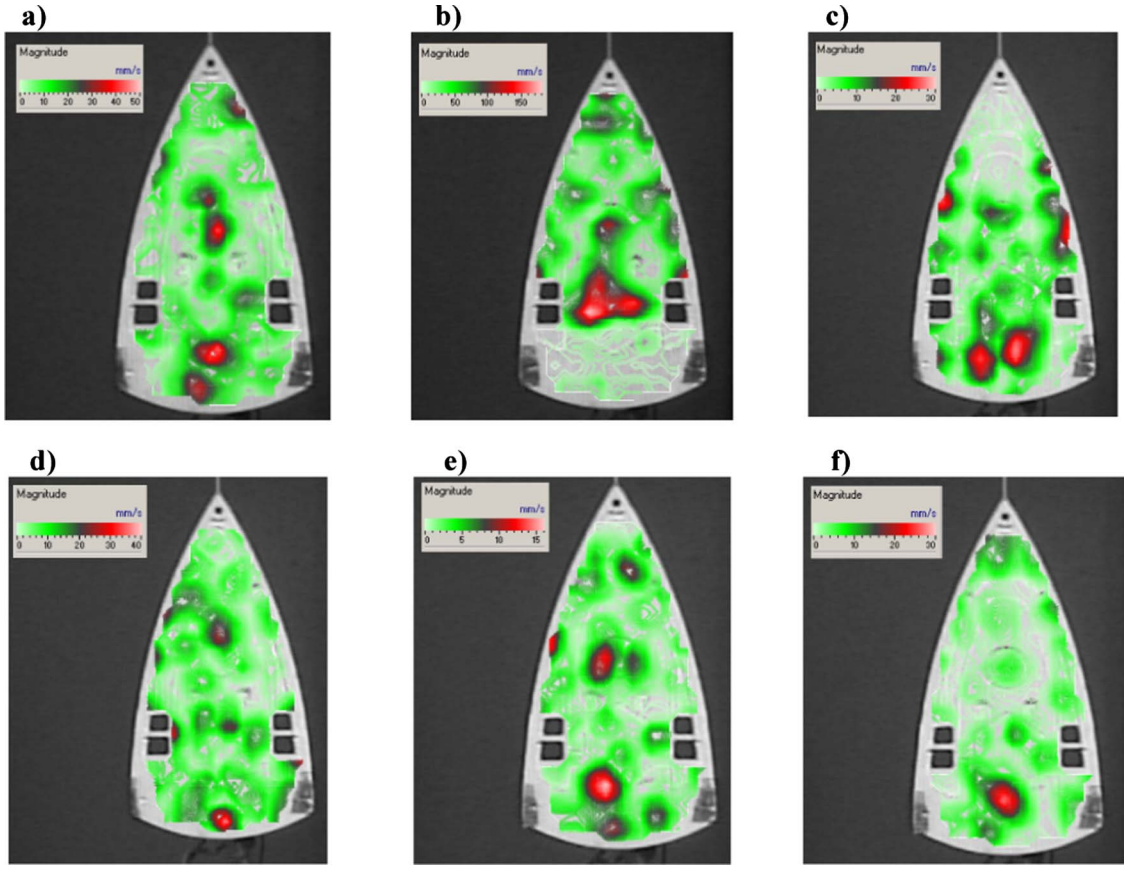

Fig. 8. Vibration shapes at frequency *f* being (a) 35 kHz, (b) 36 kHz, (c) 37 kHz, (d) 38 kHz, (e) 39 kHz and (f) 40 kHz, measured using a laser vibrometer.

vibrations and verified using a laser vibrometer here, the rest of the ultrasonic steam iron, including the electrical heating system, needs to be designed and manufactured for physical tests.

4. Conclusions

This paper presents the results of research conducted towards the realisation of designing an ultrasonic iron. After demonstrating experimental evidence that ultrasonic vibration in irons can offer significant benefits towards minimising the accumulation of limescale, a methodology for modelling, analysing and optimizing an iron structure, so as to create effective vibrations within a specified ultrasonic frequency band at desired locations, was presented.

A piezoelectric-type ultrasonic exciter with a working frequency range of 35–40 kHz was designed and optimized. A thermal isolator between the piezoelectric ceramics and iron surface was used to avoid excessive heating of the piezoelectric ceramics. In addition, a conical-shaped part was used to assemble the piezoelectric exciter with the ceramic isolator. Using finite element analyses, the ultrasonic exciter was tuned so as to set its first natural frequency corresponding to the "tension-compression" mode to be close to the desired operational frequency. The iron structure was optimized for effective ultrasonic vibrations at the operational frequency of the ultrasonic exciter. An analytical investigation of a circular plate vibration was utilized during this optimization process. Some stiffeners were also added to increase the stiffness of the shells on the iron body to prevent local modes caused by local flexibilities in the iron. As one of the design variables, the position of the ultrasonic exciter within the iron was also considered. After many simulations, a feasible ultrasonic iron structure was designed. The predicted results for the optimized iron structure indicated that the steam generating chamber, steam passageways, and the rear chamber did, in fact, vibrate effectively at ultrasonic frequencies as we had intended.

For the purpose of design validation, a prototype iron was built, and forced vibrations of this prototype at ultrasonic frequencies ranging from 35 to 40 kHz were measured using a laser vibrometer. Measurement of the operational deflection shapes confirmed the expected behaviour of the prototype. Furthermore, both predicted and measured vibration results suggested that an ultrasonic excitation, with narrowband-sweeping frequency characteristics, could provide ultrasonic vibrations at desired regions in an iron. The results of the theoretical and experimental vibration analyses as well as the physical experiments on steam irons in this study prove promising in the design of ultrasonic irons, so as to minimize the accumulation of limescale. Furthermore, we believe that ultrasonic vibrations can also improve performance by better smoothing wrinkles on fabrics and clothes. This is a topic which requires further research in the future.

Acknowledgements

The authors would like to thank to Mr. Kerem Anbarcı, Mr. Hasan İbaçoğlu and Mr. Namık Alpaydın from Aero Engineering Solutions Ltd. for their technical support. The authors also thank Dr. Caroline Fell Kurban, Director of the Center for Excellence in Learning and Teaching at MEF University for proofreading the final manuscript.

References

[1] Satake M. Chemistry for health science. New Delhi: Discovery Publishing Pvt. Ltd; 2013.
[2] Ensminger D, Bond LJ. Ultrasonics: fundamentals, technologies, and applications. third ed. Boca Raton (FL): CRC Press; 2011.
[3] Panpan L, Chen Z. Experiment study on porous fiber drying enhancement with application of power ultrasound. Appl Acoust 2017;127:169–74. http://dx.doi.org/10.1016/J.APACOUST.2017.06.003.
[4] Roopa Rani M, Rudramoorthy R. Computational modeling and experimental studies

of the dynamic performance of ultrasonic horn profiles used in plastic welding. Ultrasonics 2013;53:763–72. http://dx.doi.org/10.1016/j.ultras.2012.11.003.
[5] Fernandez Rivas D, Verhaagen B, Seddon JRT, Zijlstra AG, Jiang L-M, van der Sluis LWM, et al. Localized removal of layers of metal, polymer, or biomaterial by ultrasound cavitation bubbles. Biomicrofluidics 2012;6:34114. http://dx.doi.org/10.1063/1.4747166.
[6] Rosca I-C, Pop M-I, Cretu N. Experimental and numerical study on an ultrasonic horn with shape designed with an optimization algorithm. Appl Acoust 2015;95:60–9. http://dx.doi.org/10.1016/j.apacoust.2015.02.009.
[7] Harvey G, Gachagan A, Mutasa T. Review of high-power ultrasound-industrial applications and measurement methods. IEEE Trans Ultrason Ferroelectr Freq Control 2014;61:481–95.
[8] Tan H, Xu G, Tao T, Sun X, Yao W. Experimental investigation on the defrosting performance of a finned-tube evaporator using intermittent ultrasonic vibration. Appl Energy 2015;158:220–32. http://dx.doi.org/10.1016/j.apenergy.2015.08.072.
[9] Legay M, Simony B, Boldo P, Gondrexon N, Le Person S, Bontemps A. Improvement of heat transfer by means of ultrasound: application to a double-tube heat exchanger. Ultrason Sonochem 2012;19:1194–200. http://dx.doi.org/10.1016/j.ultsonch.2012.04.001.
[10] Jia S, Zhang D, Xuan Y, Nastac L. An experimental and modeling investigation of aluminum-based alloys and nanocomposites processed by ultrasonic cavitation processing. Appl Acoust 2016;103:226–31. http://dx.doi.org/10.1016/j.apacoust.2015.07.016.
[11] Verhaagen B, Zanderink T, Rivas DF. Ultrasonic cleaning of 3D printed objects and cleaning challenge devices. Appl Acoust 2016;103:172–81. http://dx.doi.org/10.1016/J.APACOUST.2015.06.010.
[12] Kobayashi T, Kobayashi T, Hosaka Y, Fujii N. Ultrasound-enhanced membrane-cleaning processes applied water treatments: influence of sonic frequency on filtration treatments. Ultrasonics 2003;41:185–90. http://dx.doi.org/10.1016/S0041-624X(02)00462-6.
[13] Espinoza-Beltrán FJ, Geng K, Muñoz Saldaña J, Rabe U, Hirsekorn S, Arnold W. Simulation of vibrational resonances of stiff AFM cantilevers by finite element methods. New J Phys 2009;11. http://dx.doi.org/10.1088/1367-2630/11/8/083034.
[14] Castellini P, Martarelli M, Tomasini EP. Laser Doppler vibrometry: development of advanced solutions answering to technology's needs. Mech Syst Signal Process 2006;20:1265–85. http://dx.doi.org/10.1016/j.ymssp.2005.11.015.
[15] Waldron K, Ghoshal A, Schulz MJ, Sundaresan MJ, Ferguson F, Pai PF, et al. Damage detection using finite element and laser operational deflection shapes. Finite Elem Anal Des 2002;38:193–226. http://dx.doi.org/10.1016/S0168-874X(01)00061-0.
[16] Vasiljev P, Borodinas S, Bareikis R, Struckas A. Ultrasonic system for solar panel cleaning. Sensors Actuators A Phys 2013;200:74–8. http://dx.doi.org/10.1016/j.sna.2013.01.009.
[17] Yin C, Zhang Z, Wang Z, Guo H. Numerical simulation and experimental validation of ultrasonic de-icing system for wind turbine blade. Appl Acoust 2016;114:19–26. http://dx.doi.org/10.1016/J.APACOUST.2016.07.004.
[18] Liew KM, Han J-B, Xiao ZM. Vibration analysis of circular mindlin plates using the differential quadrature method. J Sound Vib 1997;205:617–30. http://dx.doi.org/10.1006/jsvi.1997.1035.